

Article

# Importance of Rocks and Their Weathering Products on Groundwater Quality in Central-East Cameroon

Merlin Gountié Dedzo <sup>1,\*</sup>, Désiré Tsozué <sup>2</sup>, Mumbfu Ernestine Mimba <sup>3</sup>, Fulbert Teddy <sup>1</sup>, Romio Mofor Nembungwe <sup>1</sup> and Sylvie Linida <sup>1</sup>

<sup>1</sup> Department of Life and Earth Sciences, Higher Teachers' Training College, University of Maroua, P.O. Box. 55, Maroua, Cameroon; teddyfulbert@gmail.com (F.T.); moforromio@yahoo.fr (R.M.N.); linidasylvie@yahoo.com (S.L.)

<sup>2</sup> Department of Earth Sciences, Faculty of Science, University of Maroua, P.O. Box. 814, Maroua, Cameroon; tsozudsir@yahoo.fr

<sup>3</sup> Institute of Mining and Geological Research, P.O. Box 4110, Yaoundé, Cameroon; mmimba2000@yahoo.ca

\* Correspondence: merlin.gountie@gmail.com; Tel.: +237-675-088-586

Academic Editor: Luca Brocca

Received: 10 February 2017; Accepted: 30 March 2017; Published: 5 April 2017

**Abstract:** The present work highlights the influence of lithology on water quality in Méiganga and its surroundings. The main geological formations in this region include gneiss, granite and amphibolite. The soils developed on these rocks are of ABC type, which are acidic to slightly acidic. Electrical conductivity (EC), organic matter, total nitrogen, nitrate-nitrogen, sulfate, chloride, phosphorus and exchangeable base values were low to very low in the soil samples. Groundwater samples were investigated for their physicochemical characteristics. The wide ranges of EC values (15.1–436  $\mu\text{S}/\text{cm}$ ) and total dissolved solids (9–249 mg/L) revealed the heterogeneous distribution of hydrochemical processes within the groundwater of the area. The relative abundance of major dissolved species (mg/L) was  $\text{Ca}^{2+} > \text{Na}^{+} > \text{Mg}^{2+} > \text{K}^{+}$  for cations and  $\text{HCO}_3^{-} \gg \text{NO}_3^{-} > \text{Cl}^{-} > \text{SO}_4^{2-}$  for anions. All the groundwater samples were soft, with total hardness values (2.54–136.65 mg/L) below the maximum permissible limits of the World Health Organization (WHO) guideline. The majority of water samples (67%) were classified as mixed CaMg- $\text{HCO}_3$  type. Alkaline earth metal contents dominated those of alkali metals in 66.66% of samples. Thus, for the studied groundwater,  $\text{Mg}^{2+}$  and  $\text{Ca}^{2+}$  ion adsorption by clay minerals was almost nonexistent; this implies their release into the solution, which accounts for their high concentrations compared to alkali metals. Ion geochemistry revealed that water-rock interactions (silicate weathering) and ion exchange processes regulated the groundwater chemistry. One water sample points towards the evaporation domain of this diagram, indicating that groundwater probably does not originate from a deeper system. Kaolinite is the most stable secondary phase in the waters in the study area, in accordance with the geochemical process of monosiallitization, which predominated in the humid tropical zone.

**Keywords:** hydrogeochemistry; groundwater; water-rock interaction; Meiganga; East Cameroon

## 1. Introduction

The challenge of ensuring usable water in sufficient quantities to meet the needs of humans and ecosystems has emerged as one of the primary issues of the 21st century [1]. This resource is unevenly distributed and not properly managed in Cameroon and elsewhere in the world. Groundwater is an indispensable resource to sustain livelihoods in situations where the extension of the public water supply does not keep up with unregulated urbanization fueled by population growth and internal migration [2–4]. It is derived primarily by the percolation of atmospheric or surface water and it is contained in pore spaces of permeable reservoir rocks [5]. The nature of the geological formations

influences the quality of groundwater. During underground flow and depending on the residence time, there is an exchange of ions between water and rocks. The weathering of minerals in these rocks also releases mobile elements (alkali and alkaline earth) and trace elements into the waters [6,7]. These elements form an organo-metallic complex in the presence of organic matter [8].

Oxidation and precipitation of certain elements occurs upon the lowering of the groundwater level; this is the case for iron [9], silica and calcium [10]. Three principles can be proposed for the water-rock interaction [11]: (i) the chemical composition of water is controlled by the weathering of the primary minerals of the rock in the secondary phase; (ii) secondary phase formation is determined by the composition of the solutions; (iii) chemical weathering is selective because minerals do not contribute to the water composition in proportion to their modal abundances in the rocks [7].

On the African continent, Cameroon is one of the nations endowed with important fresh water resources, including surface waters (streams, rivers, lakes) and groundwater, which often discharges as springs [12]. Despite this endowment, supplies of safe drinking water are uncommon in numerous rural, peri-urban and urban areas of Cameroon. Groundwater appears, therefore, to be the most essential source of water for the population, especially in the context of climate change. Its vulnerability has been recognized as one of the most important problems in the country [13]. Approximately 70% of the population in Cameroon has access to safe drinking water [12]. On the other hand, the availability of drinking water in rural areas is only about 20% [13]. This implies that rural areas are more vulnerable to diseases related to drinking water. A comprehensive understanding of the groundwater system is necessary, therefore, for a sustainable development of this key resource, with a particular focus on rural areas. In undeveloped areas, rural water supply programs have enabled the realization of several boreholes to facilitate access to drinking water. Despite the achievement of these water points, the average number of inhabitants in rural areas to be supplied in drinking water is still high (approximately 80%) [12,13]. A great portion of the population still uses water from springs, wells and streams, the quality of which is unknown. Moreover, this quality is rarely determined, even in the case of some rural water infrastructure [14].

The main objective of this work is to contribute to a supply of better drinking water from the rock-weathering point of view in rural areas of Cameroon. More specifically, we investigate the influence of lithology on the water quality of the Méiganga area and its surroundings, by checking: (i) if there are ions that are exchanged between rock and water, and (ii) if the quantities of these elements in solution are in accordance with the WHO guideline values that would enable populations to consume the water safely. Thus, rock samples, soil samples and water samples from springs, wells and boreholes were analyzed to better understand the evolution of their qualities.

## 2. Location and Hydrogeological Background of the Study Area

Méiganga is a town of the Mbéré Division, located in the Adamawa region of Cameroon. This study area, with about 1129 km<sup>2</sup> of surface area, is situated between longitudes 14°00' and 14°25' and latitudes 06°28' and 06°43' (Figure 1), with altitudes ranging from 920 to 1200 m. The climate is sub-humid, with a mean annual rainfall of 1662 mm [15]. The rainy season extends from March to October, registering maximum rainfall in September (362 mm). The dry season stretches from November to February. The mean annual temperature is 22.6 °C [15].

From a hydrogeological point of view, the aquifers of northern Cameroon in general are poorly known; only the work of Olivry [16] gives some information on the hydrographic basin of the northern part of Cameroon. Méiganga belongs to the Mbéré hydrographic basin which is located in the Mbéré fault trough. The main river which is the Mbéré (250 km total length) has a SW-NE general direction, which is identical to that of the whole of the basin. It takes its source in the north of Méiganga at 1080 m altitude. The hydrographic network is composed of temporary and perennial streams with a dendritic network in the study area. The main tributaries are Mazoé, Boukon, Gbassoum, Kbakoungué, Mbarang and Mokombouyo, which are tributaries of the Logone River.

In the Mbéré fault trough, several authors have worked on the geology of the study area and its surrounding areas [16–21]. The geological formations of the Méiganga area and its environs represent the central part of the Panafrican belt of Cameroon, which is also called the Adamawa-Yade domain (AYD) (Figure 1b,c). The AYD covers central Cameroon, the northern Central African Republic and southern Chad; it is underlain by syn-tectonic, late-tectonic, and post-tectonic granitoids [17,18] which intrude in older metamorphic rocks. The granitoids present in the study area include biotite-muscovite granite and pyroxene–amphibole–biotite granite [19–21]. The metamorphic host rocks consist of 2.1 Ga metasediments (metamorphized conglomerates and clay sandstones) and orthogneisses, which were reworked during the Panafrican orogeny [22]. In the Méiganga area and its surroundings, these metamorphic rocks include pyroxene-amphibole gneiss, amphibole-biotite gneiss and banded amphibolite [19–21]. In the southeast of the basin, there are also small outcrops of a coarse-grained conglomerate surmounted by sandstone with upper Cretaceous clay intercalation [16].

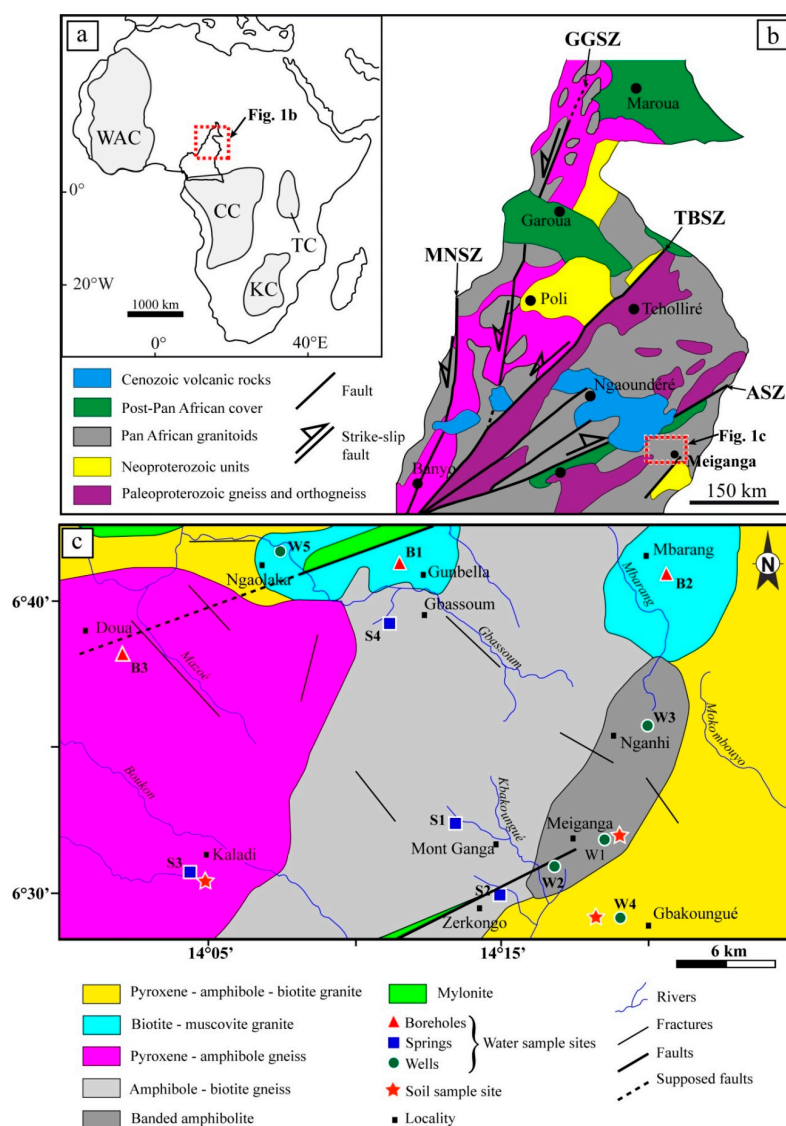


**Figure 1.** (a) Location of Cameroon in Africa, WAC: West African Craton; CC: Congo Craton; TC: Tanzanian Craton; KC: Kalahari Craton. (b) Geological sketch map of northern part of Cameroon showing from the major lithotectonic domains [17,23]; MNZ: Mayo Nolti shear zone; TBSZ: Tcholliré-Banyo Shear Zone; ASZ: Adamoua shear zone. (c) Geological map of the study area; modified from Ganwa et al. [18].

### 3. Methods of Study

#### 3.1. Sample Collection

Field studies have helped to update the geological map of the study area (Figure 1), which is composed essentially of granite, gneiss and amphibolite. This was followed by description of soils from representative profiles, dug on the three main formations, gneiss, granite and amphibolites. Soil sampling was carried out according to the methods of Baize [23]. A sampling campaign, preceded by a mapping of water points, was carried out in December 2015, to obtain an aspect of the groundwater quality from springs, wells and boreholes. Nine rock samples (four granite, four gneiss, one amphibolite), six soil samples (two on granite, two on amphibolites, two gneiss) and 12 water samples (four springs, five well, three boreholes) were collected during field work, and were prepared for laboratory analyses.

#### 3.2. Analytical Procedures

Rock samples underwent petrographic and chemical analyses. Petrographic analyses consisted of observations of rock thin sections under the polarizing microscope in order to identify the mineralogical assemblages. Rock chemical analyses for gneiss and granite have been reported in Ganwa et al. [19–21]. Only the chemical analysis of amphibolite was performed in the framework of this study. Samples were pulverized to obtain a homogeneous powder out of which 50–60 g was used for the analyses. Chemical analyses were done using the pulp at ALS Minerals Global Group, Vancouver (Canada). Whole-rock analyses for major elements were done by Inductively Coupled Plasma-Atomic Emission (ICP-AES). Loss on ignition (LOI) was determined by weight difference after ignition at 1000 °C. These analyses were used to assess their contribution in the mineralization of groundwater.

Soil analyses have allowed getting an idea on the composition of soil solution. The parameters determined include pH, electrical conductivity, organic carbon, exchangeable cations ( $\text{Ca}^{2+}$ ,  $\text{Mg}^{2+}$ ,  $\text{K}^+$ ,  $\text{Na}^+$ ), total nitrogen and available phosphorus, chlorine and sulfur. Soil pH was measured potentiometrically in a 1:2.5 soil:solution ratio. Electrical conductivity (EC) was measured in a 1:10 (solid:liquid) aqueous extract. Chloride ion was determined by potentiometric titration. Sulfate ( $\text{SO}_4^{2-}$ ) was determined by the turbidimetric method [24]. The quantity of total nitrogen was evaluated by titration after mineralization of organic matter and distillation. Exchangeable cations are shifted by ammonium acetate ( $\text{CH}_3\text{COONH}_4$ ) at pH 7. The proportions of  $\text{K}^+$  and  $\text{Na}^+$  were evaluated by flame photometry. Those of  $\text{Ca}^{2+}$  and  $\text{Mg}^{2+}$  were determined by complexometry. Organic carbon was determined by the Walkley and Black method [25]. Soil organic matter (OM) content was obtained by multiplying soil organic carbon content by 1.724 [25]. Available phosphorus was determined by the Bray-2 method [26].

For water analyses, total suspended solids (TSS) were determined by end filtration of water samples using a cellulose ester filter, with porosity of 0.45 microns, and a filtration manifold vacuum Millipore. The multi-parameter EXTIC II brand was used for the determination of the conductivity, TDS, alkalinity and pH. The pH values were read on the multi-parameter after prior calibration of the pH meter using the buffer of 7, 4 and 10 values. Chemical concentrations, including cations ( $\text{Na}^+$ ,  $\text{NH}_4^+$ ,  $\text{K}^+$ ,  $\text{Mg}^{2+}$ ,  $\text{Ca}^{2+}$ ) and anions ( $\text{F}^-$ ,  $\text{Cl}^-$ ,  $\text{NO}_3^-$ ,  $\text{PO}_4^{3-}$ ,  $\text{SO}_4^{2-}$ ) were determined by colorimetric assay using a UV-VISRS/2500 spectrophotometer. The wavelengths used for the determination of these concentrations differ from one ion to another.  $\text{HCO}_3^-$  ion was determined by titration.

### 4. Results

#### 4.1. Petrographic and Geochemical Characterisation of Geologic Formations

In detail, biotite-muscovite granite was outcropped as flagstones and/or bowls in the northern part of the study area, mostly at Ngaolaka, Gumbella and Mbarang (Figure 1c). This lithology occurred as decametric- to metric-sized amphibole-biotite gneiss enclaves, which can be found along the margins

of the Ngaolaka-Gumbella pluton. Its late- to post-tectonic character is confirmed by the discordant contact of the granite with the gneiss south of Ngaolaka. The biotite-muscovite granite is a light gray, medium- to coarse-grained porphyritic rock with K-feldspar and quartz megacrystals. It contains plagioclase, biotite, muscovite and garnet. Accessory minerals are zircon and oxides.

Pyroxene–amphibole–biotite granite crops out as flagstones and bowls at Gbakoungué, and in the west of Méiganga, Nganhi and Mbarang (Figure 1c). The rock is grayish, has a medium- to coarse-grained porphyritic texture, and contains longitudinal enclaves of amphibolite (up to 2.6 cm × 7.2 cm). Under the microscope, the rock is made up of quartz, K-feldspar, amphibole, plagioclase, biotite, and pyroxene. Accessory minerals include sphene, apatite, zircon and oxides, and secondary minerals are represented by chlorite, epidote, calcite and opaque minerals.

Amphibolite outcrops either as flagstone or bowls at Méiganga and Nganhi (Figure 1c) or as xenoliths in the pyroxene–amphibole–biotite granite. The rock is grayish, fine- to medium-grained, with a banded structure consisting of green hornblende and biotite in dark layers, and K-feldspar, plagioclase and quartz in white layers. Common accessory phases are sphene, zircon and apatite, whereas secondary minerals are opaque minerals, epidote, chlorite and calcite.

Pyroxene-amphibole gneiss and amphibole-biotite gneiss cropped out as flagstone and bowls at Doua, Kaladi, Gbassoum, Mont Ganga and Zerkongo (Figure 1c). They are gray to dark-gray in color, banded with alternate dark and white layers, and medium- to coarse-grained with a granoblastic texture and preferred orientation of the minerals. Dark layers are composed of biotite, green hornblende, pyroxene and plagioclase, while white layers comprise K-feldspar, quartz and plagioclase. Accessory minerals consist of zircon, apatite and sphene.

Rock chemical analyses are presented in Table 1. In two samples of gneiss (Ka1 and Me7) and one sample of amphibolite, the ratio of the sum of the alkaline earth metals over the alkali metals ( $(\text{MgO} + \text{CaO})/(\text{Na}_2\text{O} + \text{K}_2\text{O})$ ) is, respectively, 1.65, 1.56 and 2.70. This parameter exceeds unity and shows a dominance of alkaline earth metals ( $\text{MgO}$ : 3.22%–4.46%;  $\text{CaO}$ : 6.11%–7.15%) in relation to alkali metals ( $\text{Na}_2\text{O}$ : 2.97%–4.2%;  $\text{K}_2\text{O}$ : 1.33%–2.59%). The high contents of alkaline earth metals in these rocks indicate richness in plagioclase, pyroxene and biotite [7].

**Table 1.** Chemical analyses of sample rocks typical of the studied area.

Rocks	Px-Amph Gneiss <sup>1</sup>		Bt-Amph Gneiss <sup>2</sup>		Bt-Musc Granite <sup>3</sup>		Px Granite <sup>3</sup>		Amphibolite
Samples	Ka1	Go1	Me7	Me5	Mi2	NPg3	MB	Me6	MG
SiO <sub>2</sub>	60.72	69.30	59.41	61.66	75.46	73.45	68.8	68.34	62.73
TiO <sub>2</sub>	0.65	0.46	0.92	0.48	0.15	0.08	0.41	0.41	0.82
Al <sub>2</sub> O <sub>3</sub>	16.08	15.04	16.12	20.07	13.64	13.89	15.32	15.12	13.02
Fe <sub>2</sub> O <sub>3</sub>	6.66	4.07	7.23	3.18	1.44	0.80	3.04	3.35	6.72
MnO	0.11	0.04	0.12	0.04	0.036	0.023	0.087	0.07	0.15
MgO	3.22	1.36	3.59	1.20	0.23	0.20	1.42	1.27	4.46
CaO	6.11	2.68	5.69	2.76	0.83	0.70	1.86	2.44	7.15
Na <sub>2</sub> O	4.2	3.58	3.35	4.21	3.26	3.00	4.09	3.86	2.97
K <sub>2</sub> O	1.45	3.46	2.59	6.33	5.27	6.75	4.99	4.50	1.33
P <sub>2</sub> O <sub>5</sub>	0.2	0.19	0.26	0.22	0.05	0.13	0.19	0.19	0.18
LOI	1.02	0.59	0.92	0.75	0.59	0.25	0.64	0.92	0.59
Total	100.42	100.77	100.2	100.9	101.15	98.46	101.48	101.09	100.11
Na <sub>2</sub> O/K <sub>2</sub> O	2.90	1.03	1.29	0.67	0.62	0.44	0.82	0.86	2.23
MgO/CaO	0.53	0.51	0.63	0.43	0.28	0.29	0.76	0.52	0.62
Na <sub>2</sub> O + K <sub>2</sub> O	5.65	7.04	5.94	10.54	8.53	9.75	9.08	8.36	4.29
MgO + CaO	9.33	4.04	9.28	3.96	1.06	0.9	3.28	3.71	11.61
(MgO + CaO)/ (Na <sub>2</sub> O + K <sub>2</sub> O)	1.65	0.57	1.56	0.38	0.12	0.09	0.36	0.44	2.70

Superscripts refer to data of Toteu et al [18] (<sup>1</sup>) and Ganwa et al. [19,20] (<sup>2,3</sup>); Px: pyroxene. Bt: biotite. Amph: amphibole. Musc: muscovite.

In samples from granites and two other gneisses (Go1 and Me5), the parameter  $(\text{MgO} + \text{CaO})/(\text{Na}_2\text{O} + \text{K}_2\text{O})$  shows values ranging between 0.09 and 0.57. The value of this parameter is less than unity, and it shows a wide dominance of alkali metals ( $\text{Na}_2\text{O}$ : 3.00%–4.21%  $\text{K}_2\text{O}$ : 3.46%–6.75%) in

relation to the alkaline earth metals (MgO: 0.20%–1.42%; CaO: 0.70%–2.76%). The high concentrations of alkali metals indicate a richness of K-feldspar in the granites. In the waters,  $\text{Ca}^{2+}$  and  $\text{Na}^+$  are generally higher than  $\text{Mg}^{2+}$  and  $\text{K}^+$ , reflecting the relative abundance of the oxides CaO and  $\text{Na}_2\text{O}$  with respect to the oxides MgO and  $\text{K}_2\text{O}$  in rocks where different water samples were taken.

#### 4.2. Morphological Characteristics of Weathering Material

Morphologically, soil profiles of the study area were of ABC type. Their thicknesses varied depending on whether they were developed on gneiss, granite or amphibolites (Figure 2). From the surface to the bottom, the following horizons are noted:

- a humiferous Ap horizon. Its thickness is about 25 cm on each bedrock. It is dark, characterized by a sandy, clayey texture, a lumpy structure and high matrix porosity. Few nodules are present and there are many rootlets. The boundary is progressive and regular;
- a red B horizon. Its thickness is about 150 cm on gneiss and about 400 cm on amphibolite and granite (Figure 2). It is characterized by a clayey texture and a blocky structure. Nodules are noted on all bedrock and their contents are below 10%. The boundary is progressive and regular;
- a reddish C horizon in which the structure of the bedrock is well preserved.

Percolated water passed through the soil section before reaching the water table, which in this landscape is in the saprolite. The development of the saprolite porous network is influenced by the grain size of the minerals being dissolved. This dissolution of crystal grains by weathering produced pores, which allowed the flow of water and leaching of elements. The water quality will therefore reflect the physicochemical characteristics of the soil solution.

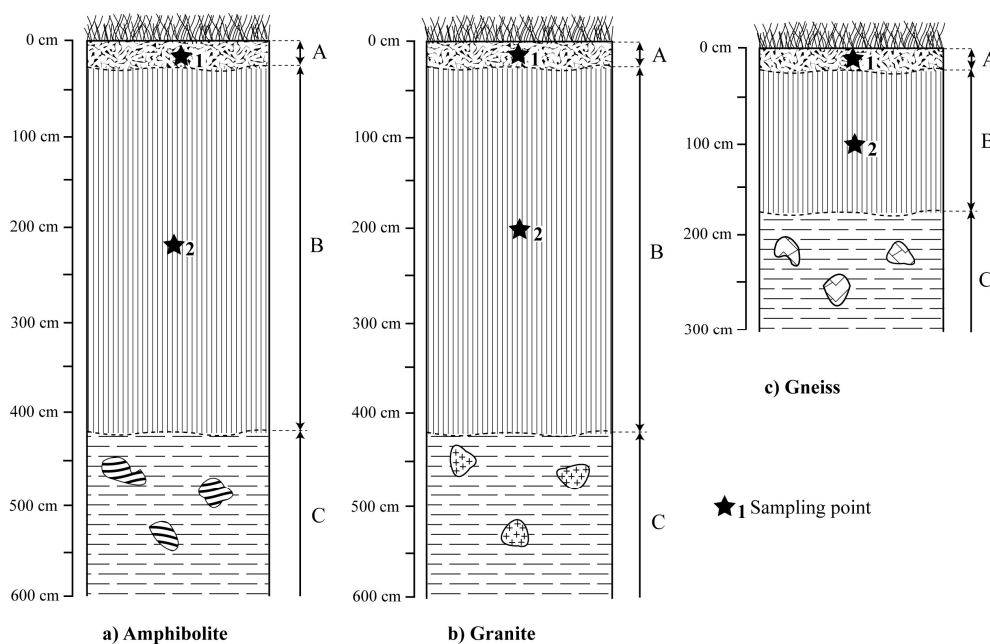


**Figure 2.** Macroscopic organization of the studied soil profile. (a) Soil profile developed on amphibolite; (b) Soil profile developed on granite; (c) Soil profile developed on gneiss.

#### 4.3. Physicochemical Characteristics of Soil Solutions

The soils are acidic to slightly acidic, with pH values ranging between 5.3 and 6.7, corresponding to a mean value of  $5.83 \pm 0.52$  ( $n = 6$ ) (Table 2). The soil pH varies slightly from one point to another, with a coefficient of variation (CV) below 15%. High values are observed on amphibolite and the lowest ones on granite. Electrical conductivity (EC) values are low, and moderately ( $15\% < \text{CV} < 35\%$ )

vary from 53 to 97  $\mu\text{S}/\text{cm}$ , corresponding to a mean value of 77.50  $\mu\text{S}/\text{cm}$  ( $n = 6$ ). Organic matter (OM) contents are low, ranging from 0.16% to 1.03%, and vary highly within the studied area ( $\text{CV} > 35\%$ ). Total nitrogen ( $\text{N}_{\text{tot}}$ ), nitrate-nitrogen ( $\text{NO}_3\text{-N}$ ), sulphate ( $\text{SO}_4^{2-}$ ) and chloride ( $\text{Cl}^-$ ) contents are very low, with mean values of 0.12%, 0.015%, 0.29% and 0.012% ( $n = 6$ ), respectively (Table 2). Their contents vary moderately within the study area. In contrast, phosphorus contents are highly variable, ranging from 2.68 to 71.48 mg/kg, with an average value of 32.66 mg/kg ( $n = 6$ ) for the studied area. Exchangeable base contents ( $\text{Ca}^{2+}$ ,  $\text{Mg}^{2+}$ ,  $\text{Na}^+$  and  $\text{K}^+$ ) are very low and highly variable, with average content largely below 1 cmol(+)/kg. There exists a significant negative correlation between P and  $\text{Na}^+$  ( $r = 0.94$ ) and between  $\text{N}_{\text{tot}}$  and  $\text{Na}^+$  ( $r = 0.95$ ). A significant positive correlation, on the contrary, is noted between  $\text{SO}_4^{2-}$  and  $\text{N-NO}_3$  ( $r = 0.94$ ), CE and  $\text{Cl}^-$  ( $r = 0.97$ ), P and  $\text{N}_{\text{tot}}$  ( $r = 0.96$ ), OM and  $\text{SO}_4^{2-}$  ( $r = 0.95$ ), OM and  $\text{N-NO}_3$  ( $r = 0.96$ ) and between  $\text{pH}_{\text{water}}$  and  $\text{pH}_{\text{KCl}}$  ( $r = 0.97$ ) (Table 3).

#### 4.4. Physicochemical Characteristics of Water Samples

The pH values of our water samples range between 5.4 and 8.12 with an average value of 6.33 ( $n = 12$ ) (Table 4). They vary slightly ( $\text{CV} < 15\%$ ) within the studied area and are essentially slightly acidic in most samples (83% of the samples). The values of the EC (15.1–436  $\mu\text{S}/\text{cm}$ ) and total dissolved solids (TDS) (9–249 mg/L) vary greatly from one sample to another ( $\text{CV} > 100\%$ ). The alkalinity (Alk) of different samples varies considerably ( $\text{CV} > 35\%$ ), with values between 122 and 1378 mg/L, and an average value of 593.83 mg/L ( $n = 12$ ). It is important to mention that the highest values of pH and alkalinity are observed in the Ngaolaka well (W5) on granite. It is also true for the Ganhi well (W3) on amphibolite, which shows the highest values of EC and TDS. On the gneiss, the values of the physical parameters are generally very low. The lowest values of the pH, EC and TDS are found in the Kaladi spring (S3).

$\text{Na}^+$  and  $\text{K}^+$  concentrations vary respectively between 1.18 and 22.05 mg/L, with a mean value of 6.07 mg/L ( $n = 12$ ), and between 0.54 and 6.74 mg/L, with an average value of 1.98 mg/L ( $n = 12$ ) (Table 4). On the other hand, the concentrations of  $\text{Mg}^{2+}$  and  $\text{Ca}^{2+}$  respectively fluctuate between 0.15 and 20.39 mg/L, with a mean value of 3.47 mg/L ( $n = 12$ ), and between 0.76 and 21.21 mg/L, with a mean value of 7.37 mg/L ( $n = 12$ ). Concentrations of  $\text{NH}_4^+$  oscillate from 0 to 0.35 mg/L with a mean value of 0.15 mg/L ( $n = 12$ ). Overall, the concentrations of cations are highly variable, with a coefficient of variation which is always greater than 35%. The highest concentrations are all measured in the Ganhi well (W3) on amphibolite, while the lowest values are found in the boreholes of Gunbella ( $\text{NH}_4^+$ : B1) and Mbarang ( $\text{Na}^+$ : B2) on granite, and in the spring of Kaladi ( $\text{Mg}^{2+}$ ,  $\text{Ca}^{2+}$ : S3) on gneiss (Table 4).

$\text{Cl}^-$  and  $\text{NO}_3^-$  are present in proportions ranging respectively between 0.03 and 33.94 mg/L (average value of 3.76 mg/L;  $n = 12$ ) and between 0.02 and 91.13 mg/L (average value of 10.77 mg/L;  $n = 12$ ). The concentrations of these ions fluctuate greatly between sample points ( $\text{CV} > 200\%$ ). The  $\text{HCO}_3^-$  contents are highly variable ( $\text{CV} > 35\%$ ) and significantly higher in all samples; they vary from 8.54 to 73.44 mg/L with a mean value of 35.51 mg/L ( $n = 12$ ). For these three ions, the highest values were all measured in the Ganhi well (W3), which is situated on amphibolite, while the lowest concentrations are found in springs situated on gneiss ( $\text{Cl}^-$ ,  $\text{NO}_3^-$ : S1;  $\text{HCO}_3^-$ : S3). The  $\text{F}^-$  and  $\text{SO}_4^{2-}$  contents vary respectively from 0.01 to 0.68 mg/L (mean value of 0.1 mg/L;  $n = 12$ ) and 0.01 to 3.45 mg/L (mean value of 0.55 mg/L;  $n = 12$ ). Their concentrations are highly variable ( $\text{CV} > 100\%$ ) in the studied area. The highest values are all measured in the wells on granite Ngaolaka (W5), whereas the lowest values are measured in the Kaladi springs on granite (S3).

The matrix of the Pearson correlations coefficients for the different variables is presented in Table 5. The data illustrate that there exists a significant positive correlation with the same value ( $r = 0.94$ ) between (i) pH and CE, TDS,  $\text{Na}^+$ ,  $\text{Ca}^{2+}$ , (ii) EC and Alk,  $\text{F}^-$ , TDS and Alk,  $\text{F}^-$ , (iii) Alk and  $\text{Na}^+$ ,  $\text{Ca}^{2+}$ , (iv)  $\text{F}^-$  and  $\text{Na}^+$ ,  $\text{Ca}^{2+}$ . A significant positive correlation with the same value ( $r = 1$ ) is also noted between (i) pH and Alk,  $\text{F}^-$ , (ii) EC and TDS,  $\text{Na}^+$ ,  $\text{Ca}^{2+}$ , (iii) TDS and  $\text{Na}^+$ ,  $\text{Ca}^{2+}$ , (iv) Alk and  $\text{F}^-$ , (v)  $\text{Na}^+$  and  $\text{Ca}^{2+}$ .

**Table 2.** Physicochemical results of soil samples.

Geologic Formations	Position	pH <sub>water</sub>	pH <sub>KCl</sub>	OC (%)	OM (%)	P (mg/kg)	EC (μS/cm)	N <sub>tot</sub> (%)	SO <sub>4</sub> <sup>2-</sup> (%)	NO <sub>3</sub> -N (%)	Cl <sup>-</sup> (%)	Ca <sup>2+</sup>	Mg <sup>2+</sup>	Na <sup>+</sup>	K <sup>+</sup>
												(cmol(+)/kg)			
Granite	1	5.3	4.5	0.60	1.03	40.14	74	0.13	0.42	0.022	0.011	1.42	0.08	0.15	0.03
	2	5.3	4.8	0.09	0.16	8.68	97	0.07	0.11	0.009	0.015	0.14	0.04	0.23	0.04
Amphibolite	1	6.3	6.1	0.55	0.94	71.48	82	0.17	0.36	0.017	0.013	0.20	0.10	0.02	0.05
	2	6.7	6.3	0.18	0.31	58.26	84	0.16	0.24	0.011	0.013	1.71	0.15	0.10	0.88
Gneiss	1	5.9	5.4	0.36	0.63	14.74	75	0.08	0.30	0.016	0.010	0.72	0.28	0.28	0.02
	2	5.5	4.7	0.36	0.63	2.68	53	0.09	0.32	0.015	0.007	0.20	0.08	0.23	0.16
Min		5.30	4.50	0.09	0.16	2.68	53.00	0.07	0.11	0.009	0.007	0.14	0.04	0.02	0.02
Max		6.70	6.30	0.60	1.03	71.48	97.00	0.17	0.42	0.022	0.015	1.71	0.28	0.28	0.88
Mean		5.83	5.30	0.36	0.62	32.66	77.50	0.12	0.29	0.015	0.012	0.73	0.12	0.17	0.20
SD		0.52	0.69	0.18	0.31	25.86	13.30	0.04	0.10	0.004	0.003	0.62	0.08	0.09	0.31
CV (%)		9.00	13.10	51.10	50.30	79.20	17.20	33.40	33.60	28.00	22.30	85.50	64.10	52.60	157.20

Max: maximum; Min: minimum; SD: standard deviation; CV: Coefficient of variation; OC: Organic carbon; OM: Organic matter; EC: electrical conductivity; N<sub>tot</sub>: Total Nitrogen.

**Table 3.** Pearson's correlation coefficients for physicochemical parameters of soil samples.

	pH <sub>eau</sub>	pH <sub>KCl</sub>	CO	MO	P	EC	N <sub>tot</sub>	SO <sub>4</sub> <sup>2-</sup>	NO <sub>3</sub> -N	Cl <sup>-</sup>	Ca <sup>2+</sup>	Mg <sup>2+</sup>	Na <sup>+</sup>	K <sup>+</sup>
pH <sub>eau</sub>	1													
pH <sub>KCl</sub>	0.977 *	1												
CO	-0.090	-0.112	1											
MO	-0.097	-0.121	1.000 *	1										
EG	0.199	0.064	-0.129	-0.121										
P	0.711	0.731	0.391	0.376	1									
CE	0.172	0.317	-0.442	-0.454	0.304	1								
N <sub>tot</sub>	0.705	0.682	0.425	0.412	0.967 *	0.100	1							
SO <sub>4</sub> <sup>2-</sup>	0.022	-0.061	0.953 *	0.955 *	0.371	-0.605	0.459	1						
NO <sub>3</sub> -N	-0.227	-0.279	0.958 *	0.960 *	0.235	-0.480	0.274	0.946 *	1					
Cl <sup>-</sup>	0.223	0.364	-0.375	-0.389	0.429	0.979 *	0.250	-0.540	-0.448	1				
Ca <sup>2+</sup>	0.368	0.236	0.070	0.065	0.411	0.062	0.447	0.255	0.214	0.069	1			
Mg <sup>2+</sup>	0.426	0.387	0.033	0.041	-0.005	-0.118	-0.075	0.146	0.102	-0.254	0.271	1		
Na <sup>+</sup>	-0.590	-0.620	-0.382	-0.366	-0.944 *	-0.231	-0.952 *	-0.335	-0.184	-0.400	-0.214	0.292	1	
K <sup>+</sup>	0.716	0.606	-0.440	-0.447	0.387	0.107	0.474	-0.224	-0.440	0.162	0.643	0.109	-0.326	1

\* Significant at  $p < 0.05$ .

**Table 4.** Physicochemical results of water samples.

Geologic Formations	Locality	Sample ID	pH	EC	TDS	TSS	Alk.	F <sup>-</sup>	Cl <sup>-</sup>	NO <sub>3</sub> <sup>-</sup>	PO <sub>4</sub> <sup>3-</sup>	SO <sub>4</sub> <sup>2-</sup>	HCO <sub>3</sub> <sup>-</sup>	Na <sup>+</sup>	K <sup>+</sup>	Mg <sup>2+</sup>	Ca <sup>2+</sup>	NH <sub>4</sub> <sup>+</sup>	TH
			UC	μS/cm	mg/L	mg/L	mg/L	mg/L	mg/L	mg/L	mg/L	mg/L	mg/L	mg/L	mg/L	mg/L	mg/L	mg/L	mg/L
Ampibolite	Mokolo	W1	6.31	215	123	65.2	736	0.06	9.34	34.22	0	1.81	44.90	12.23	3.41	5.80	16.83	0.21	65.86
	Kpok-ko	W2	5.88	40.1	23	21.6	303	0.05	0.72	1.11	0	0.05	18.48	3.20	1.31	0.93	2.36	0.22	9.72
	Ganhi	W3	6.33	436	249	21.2	723	0.10	33.94	91.13	0	0.66	73.44	22.05	6.74	20.39	21.21	0.35	136.65
Granite	Gbakoungué	W4	5.93	20.4	12	11.6	156	0.03	0.13	1.34	0	0.08	9.52	1.46	0.54	0.35	1.79	0.23	5.92
	Ngaolaka	W5	8.12	136.2	78	13.2	1378	0.68	0.47	0.06	0	3.45	8.62	9.21	2.55	0.74	16.69	0.26	44.79
	Gunbella	B1	5.93	34.2	20	16	307	0.04	0.05	0.06	0.01	0.09	19.48	1.57	0.94	1.10	2.80	0	11.51
	Mbarang	B2	5.92	21.4	12	26.8	122	0.02	0.07	0.14	0.03	0.13	45.90	1.18	2.45	0.25	0.99	0.06	3.49
Gneiss	Mont ganga	S1	7.2	102.4	59	15.2	1183	0.06	0.03	0.02	0	0.01	72.16	6.34	0.66	4.48	8.52	0.11	39.67
	Zerkongo	S2	6.53	94.1	54	14.4	876	0.07	0.16	0.03	0.02	0.09	53.44	7.05	1.11	2.54	8.46	0.15	31.56
	Kaladi	S3	5.4	15.1	9	15.2	140	0.01	0.08	0.02	0.09	0.01	8.54	1.43	0.69	0.15	0.76	0.10	2.54
	Gbassoum	S4	6.08	56.6	32	16.2	534	0.05	0.04	1.01	0	0.13	63.16	2.85	0.84	2.91	3.80	0.06	21.46
	Doua	B3	6.31	69.5	40	13.6	668	0.07	0.06	0.12	0.27	0.14	8.54	4.25	2.55	1.96	4.26	0	18.66
WHO Standard (2004)	DL		6.5–8.5	500	500	-	-	-	200	10	5	200	200	<20	12	50	75	-	100
	PL		9.2	1400	1000	1500	200	1.5	600	50	50	400	300	200	100	150	200	0.5	500
<b>Statistical data</b>																			
	Min		5.4	15.1	9	11.6	122	0.01	0.03	0.02	0	0.01	8.54	1.18	0.54	0.15	0.76	0	2.54
	Max		8.12	436	249	65.2	1378	0.68	33.94	91.13	0.27	3.45	73.44	22.05	6.74	20.39	21.21	0.35	136.65
	Mean		6.33	103.42	59.25	20.85	593.83	0.1	3.76	10.77	0.08	0.55	35.51	6.07	1.98	3.47	7.37	0.15	32.65
	SD		0.68	114.67	65.45	13.99	395.26	0.17	9.45	25.96	0.08	1.00	24.94	5.87	1.70	5.38	6.80	0.11	36.38
	CV (%)		11	111	110	67	67	167	251	241	220	180	70	97	86	155	92	72	111.40

W: wells; S: springs; B: boreholes; EC: electrical conductivity; TDS: total dissolved solids; TSS: total suspended solids; Alc: alkalinity; DL and PL stand for desired limit and max permissible limit, respectively; Max: maximum; Min: minimum; SD: standard deviation; CV: coefficient of variation; TH: total hardness (as CaCO<sub>3</sub> in mg/L) = 2.5(Ca<sup>2+</sup>) + 4.1(Mg<sup>2+</sup>).

**Table 5.** Pearson's correlation coefficients for physicochemical parameters of water samples.

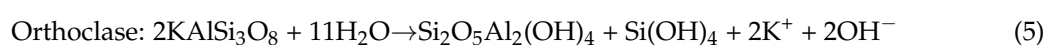
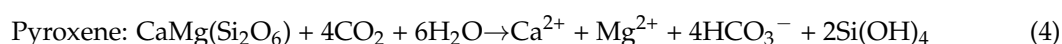
	pH	EC	TDS	TSS	Alk	F <sup>-</sup>	Cl <sup>-</sup>	NO <sub>3</sub> <sup>-</sup>	PO <sub>4</sub> <sup>3-</sup>	SO <sub>4</sub> <sup>-</sup>	HCO <sub>3</sub> <sup>-</sup>	Na <sup>+</sup>	NH <sub>4</sub> <sup>+</sup>	K <sup>+</sup>	Mg <sup>2+</sup>	Ca <sup>2+</sup>
T																
pH	1															
EC	0.943 *	1														
TDS	0.943 *	1.000 *	1													
TSS	-0.600	-0.371	-0.371	1												
Alk	1.000 *	0.943 *	0.943 *	-0.600	1											
F <sup>-</sup>	1.000 *	0.943 *	0.943 *	-0.600	1.000	1										
Cl <sup>-</sup>	0.543	0.600	0.600	0.086	0.543	0.543	1									
NO <sub>3</sub> <sup>-</sup>	0.086	0.314	0.314	0.657	0.086	0.086	0.257	1								
PO <sub>4</sub> <sup>3-</sup>	-0.516	-0.516	-0.516	0.030	-0.516	-0.516	-0.213	-0.334	1							
SO <sub>4</sub> <sup>-</sup>	0.829	0.771	0.771	-0.314	0.829	0.829	0.829	0.200	-0.273	1						
HCO <sub>3</sub> <sup>-</sup>	-0.143	0.086	0.086	0.771	-0.143	-0.143	0.143	0.771	-0.577	-0.143	1					
Na <sup>+</sup>	0.943 *	1.000 *	1.000 *	-0.371	0.943 *	0.943 *	0.600	0.314	-0.516	0.771	0.086	1				
NH <sub>4</sub> <sup>+</sup>	0.609	0.667	0.667	0.174	0.609	0.609	0.638	0.609	-0.832	0.638	0.609	0.667	1			
K <sup>+</sup>	0.600	0.714	0.714	-0.086	0.600	0.600	0.829	0.257	0.091	0.771	-0.086	0.714	0.348	1		
Mg <sup>2+</sup>	0.371	0.600	0.600	0.086	0.371	0.371	-0.029	0.600	-0.395	0.029	0.486	0.600	0.348	0.257	1	
Ca <sup>2+</sup>	0.943 *	1.000 *	1.000 *	-0.371	0.943*	0.943*	0.600	0.314	-0.516	0.771	0.086	1.000 *	0.667	0.714	0.600	1

\* Significant at  $p < 0.05$ .

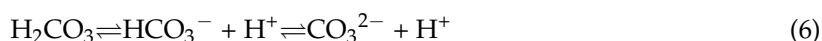
## 5. Discussion

The range of water pH values reveals that the samples were generally weakly acidic to neutral. This weakly acidic to neutral pH could be attributed to the influence of organic matter in the overlying soil [1]. Despite their relatively low pH values below the WHO guideline value, TDS and EC exhibited a wide range. The high standard deviation of 65.45 and 114.67 for TDS and EC, respectively, indicates the heterogeneity of the hydrochemical processes evolving within the groundwater of the Méiganga area [27,28]. Nevertheless, all the investigated samples were fresh (TDS < 1000 mg/L), and, for the most part (10 samples over 12), soft (TH < 60 mg/L) [29]; the two other investigated water samples (W1 and W3) situated on amphibolite were moderately hard, with TH = 65.86 and 136.65 mg/L, respectively. All the groundwater samples had hardness below the maximum permissible limits of the WHO guideline. The alkalinity values are nearly all (nine samples over 12) above the WHO guideline value. It is the quantitative capacity of an aqueous solution to neutralize an acid, which is commonly known as the “buffering capacity”. Alkalinity indicates the ability for groundwater to neutralize the inputs of acidity, and generally consists of the bicarbonate (HCO<sub>3</sub>) and the carbonate (CO<sub>3</sub><sup>2-</sup>) concentration. High alkalinity values might lead to a high buffering capacity [30]. The well of the Ganhi locality (W3) showed a concentration of NO<sub>3</sub><sup>-</sup> above the maximum acceptable limits. This value of NO<sub>3</sub><sup>-</sup>, recorded in the shallowest well (about 6.5 m), is located in a densely populated area, and therefore might be linked to anthropogenic activities. This statement is comparable with recent studies of Kamtchueng et al. [28], Wirmvem et al. [31] and Ako et al. [32] on groundwater in the Monoun, Ndop and Banana localities in Cameroon, respectively, where sewage sludge, effluent, agriculture and spreading of animal manure were identified as the plausible causes of the increasing levels of nitrate in groundwater. Owing to the absence of a significant correlation between NO<sub>3</sub><sup>-</sup> and K<sup>+</sup> (r = 0.25), agricultural practices cannot be considered as the main source of NO<sub>3</sub><sup>-</sup> in the Méiganga area. All other chemical parameters of the analyzed groundwater samples were found to be acceptable based on the WHO guideline value [33].

The chemical composition of the water samples was identified and classified using the trilinear plot described by Piper [34], and the data are presented on Figure 3a. This plot shows that eight samples belong to the CaMg-HCO<sub>3</sub> domain, and four other samples belong to the CaMg-Cl or CaMg-SO<sub>4</sub> domains, chemically dominated by alkaline earth metals (Ca<sup>2+</sup> and Mg<sup>2+</sup>). The last two samples belong to the Na + K-HCO<sub>3</sub> domain. Na<sup>+</sup> and K<sup>+</sup> concentrations represented approximately 42.62% of the sum of the major cations (Figure 3b). In the same way, the sum of Cl<sup>-</sup>, nitrate NO<sub>3</sub><sup>-</sup>, and SO<sub>4</sub><sup>2-</sup> represented, on average, roughly 30% of the total anions in all samples, while HCO<sub>3</sub><sup>-</sup> constituted about 70% (Figure 3b). The predominance of HCO<sub>3</sub> suggests that intense chemical weathering processes are taking place in this aquifer. Natural processes such as the incongruent dissolution of silicates in the rocks that react with CO<sub>2</sub> gas from root or microorganism respiration and from the mineralization of soil organic matter could be a mechanism that releases Ca, Mg, Na, K and HCO<sub>3</sub> into the groundwater, as indicated in the following reactions [35–38]:



The action of microorganisms contained in the soil through the degradation of vegetable matter also plays a significant role in the formation of bicarbonate ions according to the following equation:



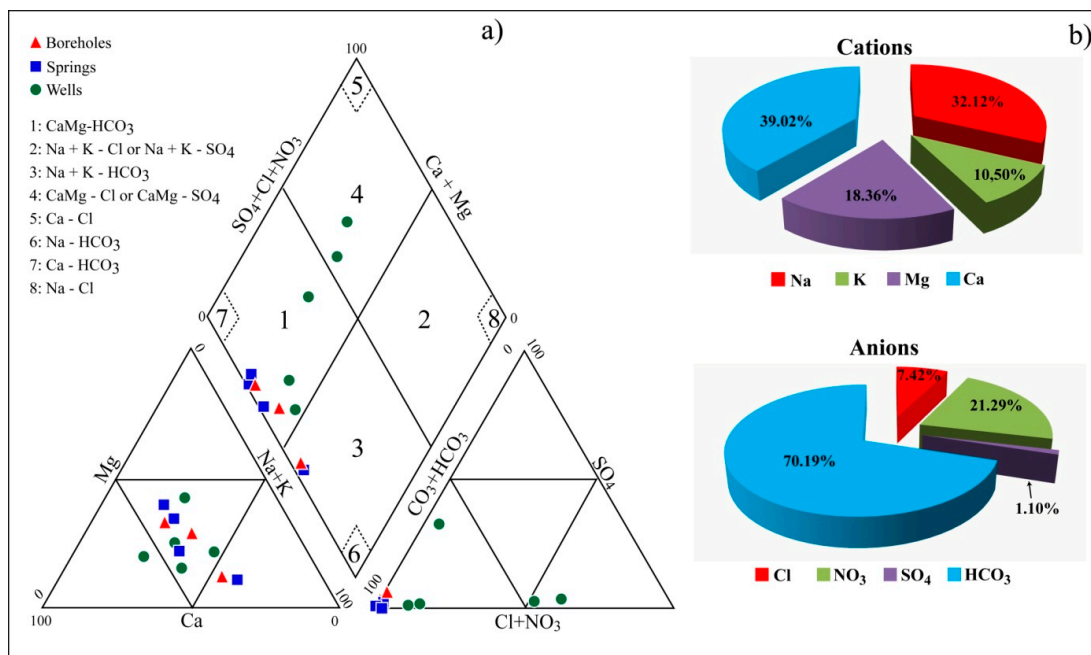


**Figure 3.** (a) Piper [33] trilinear diagram describing the chemical composition of water samples for the studied area. (b) Pie chart of mean concentrations of ions (mg/L) showing alkaline earth metals (Ca + Mg) exceed alkali metals (Na + K), and weak acids ( $\text{CO}_3 + \text{HCO}_3$ ) greatly exceed strong acids ( $\text{SO}_4 + \text{Cl}$ ).

Along the Cameroon Volcanic Line [7,39,40] and elsewhere in other countries [41,42], analogous observations have been reported in springs. Those observations are confirmed by the Gibbs diagram [43] for the study area (Figure 4a,b) which indicates that water-rock interaction is the dominant process controlling the main chemical composition of groundwater. Only one sample points towards the evaporation domain, indicated that groundwater does not likely originate from a deeper system [31]. Major ions of groundwater in the study area are thus derived from the weathering of minerals in host rocks.

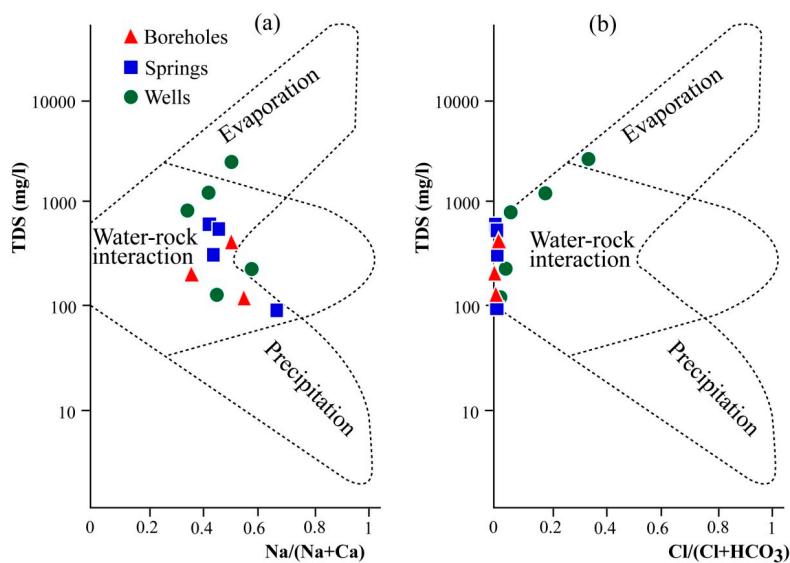


**Figure 4.** Gibbs [42] plots indicating water-rock interaction as the main process regulating the chemistry of waters in the study area. (a) TDS versus  $\text{Na}/(\text{Na}+\text{Ca})$  diagram; (b) TDS versus  $\text{Cl}/(\text{Cl}+\text{HCO}_3)$ .

The use of activity diagrams (Figure 5) of the alkaline earth metals and the alkali metals [44] allows the identification of secondary minerals that are in equilibrium or nearly in equilibrium with the analyzed waters. This diagram was drawn assuming a temperature of 25 °C and a pressure of 1 atm, using the DIAGRAMME computer program. It indicates that most of the samples belong to the kaolinite stability field, demonstrating that kaolinite is the most stable secondary phase for the waters in the study area. This result is consistent with what has been reported by some authors [7,28,31,39,40] under humid tropical climatic conditions. Kaolinite constituted the main clay mineral formed through the monosialitization process, which characterizes the humid tropical zone [45]. One sample (W5) plotted in the illite stability field was a mineral that has been pointed out in the humid tropical zone by many authors [46–48]. Illite might derive from the transformation of micas contained in granite rock [49].

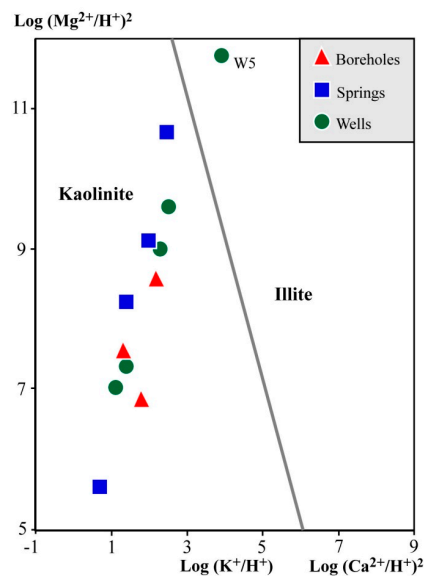


Figure 5. Plots of various water sources in the Korjinski [43] diagram.

The compositional relations between the dissolved ions (Table 6) were computed using stoichiometric relations. The  $(Ca + Mg)/\text{total cations}$  ratios of all the samples varied from 0.36 to 0.75, with 83% of the values higher than 0.5, implying a high contribution of  $Ca^{2+}$  and  $Mg^{2+}$  in cations [28,50]. Further, the plot of  $(Ca + Mg)$  versus total cations for all the water samples (Figure 6a) showed that the whole points were below the 1:1 line, suggesting a contribution from the weathering reactions. Moreover, the dispersion of points around the 1:1 line on the  $(Ca^{2+} + Mg^{2+})$  versus  $(HCO_3^- + SO_4^{2-})$  plot (Figure 6b) indicates that  $Ca^{2+}$  and  $Mg^{2+}$  enrichment in waters does not originate from the dissolution of carbonate minerals [28,51]; this statement result confirms that the weathering of silicates is the main source of the alkaline earth metals in waters. The  $(Na + K)/\text{total cations}$  ratios range from 0.25 to 0.61, with 83% of the values less than 0.5, suggesting that weathering of silicate minerals is the source of major cations in groundwater in the study area [52]. The  $Na/Cl$  ratio is equal to one in the groundwater when these two ions derive from the dissolution of halite in salt horizons [53]. This ratio, which oscillates from one to 280, was overall greater than one and higher than that of seawater (0.86), indicating the occurrence of an ion exchange process in the aquifer that is different from halite dissolution. Sodium feldspar (albite) dissolution (Reaction (2)) is thus likely to be one of the geochemical processes responsible for liberating extra  $Na^+$  into the solution, leading to  $Na^+/Cl^-$  ratios higher than that of seawater. Nevertheless, the  $Cl^-$  deficiency over  $Na$  appears to indicate that  $Cl^-$  in the samples could be derived from rainwater. This process, also described by Kamtchueng et al. [27] in the Lake Nyos catchment (West Cameroon), may happen when rainwater dissolves chloride ions in wind-driven aerosols from the atmosphere.

**Table 6.** Stoichiometric relations between some solutes in the water samples.

Geologic Formations	Sample ID	(Ca + Mg)/ Total Cations	(Na + K)/ Total Cations	(Ca + Mg)/ (HCO <sub>3</sub> + SO <sub>4</sub> )	(Ca + Mg)/ HCO <sub>3</sub>	Na/Cl	Na/Ca
Ampibolite	W1	0.68	0.32	1.69	1.78	2.04	0.63
	W2	0.53	0.45	0.67	0.67	7.00	1.17
	W3	0.70	0.29	2.26	2.28	1.00	0.91
Granite	W4	0.60	0.35	0.75	0.75	15.00	0.67
	W5	0.65	0.34	4.24	6.36	30.77	0.48
	B1	0.72	0.28	0.72	0.72	70	0.50
	B2	0.39	0.61	0.09	0.09	25	1.00
Gneiss	S1	0.72	0.27	0.67	0.67	280	0.67
	S2	0.64	0.35	0.72	0.72	62	0.74
	S3	0.36	0.57	0.36	0.36	30	1.50
	S4	0.75	0.25	0.41	0.41	120	0.63
	B3	0.59	0.41	2.64	2.64	95	0.90
<b>Statistical data</b>							
Min		0.36	0.25	0.09	0.36	1	0.48
Max		0.75	0.61	4.24	6.36	280	1.50
Mean		0.61	0.37	1.27	1.45	61.48	0.82
SD		0.12	0.11	1.16	1.66	75.25	0.28
CV		19.90	29.70	92.20	114.40	122.4	34.9

The ratios of dissolved ions are computed using meq/L value.

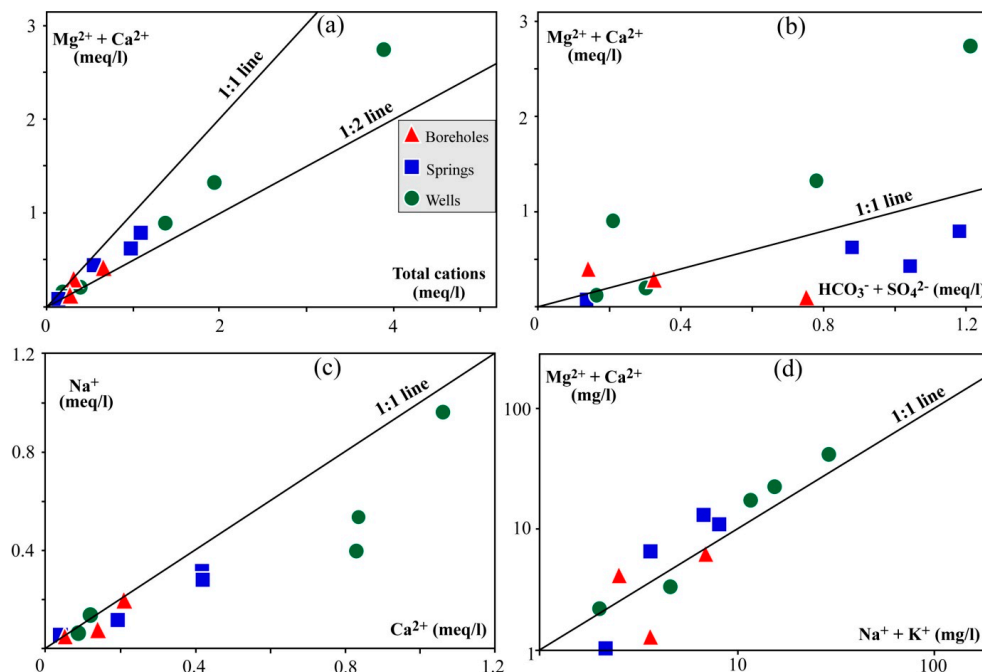


**Figure 6.** Cross-plots showing the interrelationship among dissolved species: (a) ( $Mg^{2+} + Ca^{2+}$ ) vs. Total cations; (b) ( $Mg^{2+} + Ca^{2+}$ ) vs. ( $HCO_3^- + SO_4^{2-}$ ); (c)  $Na^+$  vs.  $Ca^+$ ; (d) ( $Mg^{2+} + Ca^{2+}$ ) vs. ( $Na^+ + Ca^+$ ) diagram, modified after Henry and Wassenaar [54].

The ion exchange process is also verified by the  $Na^+/Ca^{2+}$  ratio (0.48–1.50) and the Na versus Ca diagram (Figure 6c), in which the great majority of water samples are plotted below the 1:1 line [27–52].

The process of ion exchange is defined as indirect when  $Ca^{2+}$  or  $Mg^{2+}$  in groundwater is replaced by Na or K from the rock, and as direct when Na or K in groundwater is replaced by Ca or Mg [54–56]. Eight samples of 12 display a  $Ca + Mg/HCO_3 + SO_4$  ratio  $<1$ , demonstrating the indirect type of base-exchange reaction, which involves the liberation of Na or K into groundwater and the adsorption

of Ca or Mg by clay minerals. Nevertheless, the geological setting characterized fractured rocks and faults, and the high slope gradient of the study area may favor the rapid circulation of the water. This very limited residence time of water in geological formations does not favor the development of ion exchange [27], reflecting the dominance of the alkaline earth metals in water. To verify this last assertion, the positioning of the analyzed waters in the Hendry and Wassenaar [57] diagram (Figure 6d) helps to understand the behavior of alkaline earth metals and the alkali metals in the waters. It emerges that only four samples are found below the 1:1 equiline, indicating that the alkali metals are relatively more abundant than the alkaline earth metals in the four samples; the leaching and the adsorption phenomenon of  $Mg^{2+}$  and  $Ca^{2+}$  ions in the clay mineral lattices influence this trend. On the other hand, most of the samples (eight) are plotted above the 1:1 line, showing that the alkaline earth metal contents dominated those of alkali metals in these samples; thus, for the studied groundwater,  $Mg^{2+}$  and  $Ca^{2+}$  ion adsorption by clay minerals is almost nonexistent. This implies their release into solution, which accounts for their high concentrations compared to alkali metals.

## 6. Conclusions

The hydrogeochemical studies of groundwater in Méiganga and the surrounding areas revealed that the water samples were generally slightly acidic to neutral ( $5.3 < \text{pH} < 6.7$ ), fresh ( $\text{TDS} < 1000 \text{ mg/L}$ ), soft and moderately hard ( $2.54 < \text{TH} < 136.65 \text{ mg/L}$ ). The CaMg- $\text{HCO}_3$  type were the most dominant water variety in the study area, whereas the CaMg-Cl and CaMg- $\text{SO}_4$  types were less represented. Petrographic and geochemical studies, coupled with soil and hydrogeochemical results, showed that the dominant factors controlling the water chemistry in the area are anthropogenic activities, water-rock interactions (chemical weathering) and ion exchange. Adsorption of  $Mg^{2+}$  and  $Ca^{2+}$  ions by clay minerals was almost nonexistent; their release into solution accounts for their high concentrations compared to alkali metals in our groundwater samples. Major ions of groundwater in the study area are thus derived from the weathering of minerals contained in host rocks. Only one sample trended towards the evaporation domain of the Gibbs diagram, indicating that groundwater probably does not originate from a deeper system. High values of nitrate above the WHO guideline values were due to anthropogenic activities. The activity diagram for alkaline earth metals and alkali metals indicated that most of the samples belong to the kaolinite stability field, demonstrating that kaolinite is the most stable secondary phase for the waters in the study area.

**Acknowledgments:** Our sincere thanks to P. Azinwi Tanful and M.J. Wirmvem for their constructive comments and English revision which contributed to improve this paper. We also thank the two anonymous referees for their constructive remarks that substantially improved the ideas stated in the paper.

**Author Contributions:** M. Gountié Dedzo and D. Tsozué designed research and wrote the manuscript. M.E. Mimba, F. Teddy, R. Mofor Nembungwe and S. Linida contributed for editing the manuscript and gave constructive comments and suggestions.

**Conflicts of Interest:** The authors declare no conflict of interest.

## References

1. Oki, A.O.; Akana, T.S. Quality Assessment of Groundwater in Yenagoa, Niger Delta, Nigeria. *Geosciences* **2016**, *6*, 1–12.
2. Ndiomo, E.D.; Mengue Mbom, A.; Assako Assako, R. Remote sensing and rational interventions for the urban development in Africa. The case of Yaounde in Cameroon (Central Africa). In Proceedings of the ISPRS, Tempe, AZ, USA, 14–16 March 2005; p. 5.
3. Ngnikam, E.; Mougoue, B.; Tietche, F. Eau, Assainissement et impact sur la santé: Étude de cas d'un écosystème urbain à Yaoundé. In Proceedings of the Actes des JSIRAUF, Hanoi, Vietnam, 6–9 November 2007.
4. Kringel, R.; Rechenburg, A.; Kuitcha, D.; Fouépé, A.; Bellenberg, S.; Kengne, I.M.; Fomo, M.A. Mass balance of nitrogen and potassium in urban groundwater in Central Africa, Yaounde/Cameroon. *Sci. Total Environ.* **2016**, *547*, 382–395. [[CrossRef](#)] [[PubMed](#)]
5. Ayoade, J.O. *Tropical Hydrology and Water Resources*; Macmillan Ltd.: London, UK, 2003; p. 276.

6. Salbu, B.; Steinnes, E. *Trace Elements in Natural Water*; CRC Press. Inc.: Boca Raton, FL, USA, 1995; p. 302.
7. Nono, A.; Temgoua, E.; Likeng, J.D.H.; Djoukoko, T.J.P. Influence de la nature lithologique et des structures géologiques sur la qualité des eaux souterraines dans le versant Nord des Monts Bambouto: Cas du village Balepo et ses environs. *Afr. Geosci. Rev.* **2008**, *15*, 149–162.
8. Jackson, T.A. The Biogeochemical and Ecological Significance of Interactions between Colloidal Minerals and Trace Elements. In *Environmental Interactions of Clays*; Rae, J., Parker, A., Eds.; Springer: Berlin/Heidelberg, Germany, 1998; p. 273.
9. Temgoua, E.; Djeuda, T.H.B.; Tanawa, E.; Guenat, C.; Pfeifer, H.R. Groundwater fluctuations and footslope ferricrete soils in the humid tropical zone of southern Cameroon. *Hydrol. Proc.* **2005**, *19*, 3097–3111. [[CrossRef](#)]
10. Nahon, D. *Cuirasses Ferrugineuses et Encroûtement Calcaires au Sénégal Occidental et en Mauritanie. Système Évolutifs: Géochimie, Structures, Relais et Coexistence*; Mémoire Société Géologique: Strasbourg, France, 1976; p. 232.
11. Drever, J.I.; Zobrist, S. Chemical weathering of silicate rocks as a function of evolution in the southern Swiss Alps. *Geochim. Cosmochim. Acta* **1992**, *56*, 3209–3216. [[CrossRef](#)]
12. World Health Organization and United Nations Children’s Fund (WHO/UNICEF). Coverage Estimates: Improved Sanitation, Cameroon. Joint Monitoring Programme for Water Supply and Sanitation. 2008. Available online: [http://documents.wssinfo.org/download/id\\_document](http://documents.wssinfo.org/download/id_document) (15 September 2008).
13. Ako, A.A.; Takem, E.G.E.; Nkeng, E.G. Water resources management and integrated water resources management (IWRM) in Cameroon. *Water Resour. Manag.* **2010**, *24*, 871–888. [[CrossRef](#)]
14. Djeuda, T.H.B.; Tanawa, E.; Ngnikam, E. *L’eau au Cameroun; Tome I: Approvisionnement en Potable*; Presse Universitaire Yaoundé: Yaoundé, Cameroun, 2001; p. 359.
15. Suchel, J.B. Les Climats du Cameroun. Tome III. Ph.D. Thesis, Université de St Etienne, St. Etienne, France, 1987; p. 1186.
16. Olivry, J.C. *Fleuves et Rivières du Cameroun*; Collection “Monographies Hydrologiques ORSTOM”; ORSTOM: Marseille, France, 1986; p. 547.
17. Lasserre, M. *Carte Géologique de Reconnaissance à L’échelle 1/500 000, Territoire du Cameroun, Ngaoundéré-Est, Dir*; Mines Géol. Cameroun: Yaoundé, Cameroun, 1961.
18. Toteu, S.F.; Van Schmus, R.W.; Penaye, J.; Michard, A. New U–Pb and Sm–Nd data from North-Central Cameroon and its bearing on the Pre-Pan-African history of Central Africa. *Precamb. Res.* **2001**, *108*, 45–73. [[CrossRef](#)]
19. Ganwa, A.A.; Frisch, W.; Siebel, W.; Shang, K.C.; Ondo, M.J.; Satir, M.; Numbem, T.J. Zircon 207Pb/206Pb evaporation ages of Pan-African metasedimentary rocks in the Kombé-II area (Bafia Group, Cameroon): Constraints on protolith age and provenance. *C. R. Géosci.* **2008**, *340*, 211–222. [[CrossRef](#)]
20. Ganwa, A.A.; Siebel, W.; Frisch, W.; Kongnyuy Shang, C. Geochemistry of magmatic rocks and time constraints on deformational phases and shear zone slip in the Méiganga area, central Cameroon. *Int. Geol. Rev.* **2011**, *53*, 759–784. [[CrossRef](#)]
21. Ganwa, A.A.; Siebel, W.; Kongnyuy Shang, C.; Seguem, N.; Ekodeck, G.E. New Constraints from Pb-Evaporation Zircon Ages of the Méiganga Amphibole-Biotite Gneiss, Central Cameroon, on Proterozoic Crustal Evolution. *Int. J. Geosci.* **2011**, *2*, 138–147.
22. Toteu, S.F.; Penaye, J.; Poudjom-Djomani, Y. Geodynamic evolution of the Pan-African belt in central Africa with special reference to Cameroon. *Can. J. Earth Sci.* **2004**, *41*, 73–85. [[CrossRef](#)]
23. Baise, D. *Guide pour la Description des Sols*; Institut National de la Recherche Agronomique (INRA): Paris, France, 1995.
24. Verma, B.C.; Swaminathan, K.; Sud, K.C. An improved turbidimetric procedure for determination of sulphate in plants and soils. *Talanta* **1977**, *29*, 49–50. [[CrossRef](#)]
25. Walkey, A.; Black, I.A. Determination of organic matter in soil. *Soil Sci.* **1934**, *37*, 549–556.
26. Bray, R.H.; Kurtz, L.T. Determination of total organic and available forms of phosphorus in soils. *Soil Sci.* **1945**, *59*, 22–229. [[CrossRef](#)]
27. Kamtchueng, B.T.; Fantong, W.Y.; Ueda, A.; Tiodjio, E.R.; Anazawa, K.; Wirmvem, M.J.; Mvondo, J.O.; Nkamdjou, S.L.; Kusakabe, M.; Ohba, T.; et al. Assessment of shallow groundwater in Lake Nyos catchment (Cameroon, Central-Africa): Implications for hydrogeochemical controls and uses. *Environ. Earth Sci.* **2014**, *72*, 3663–3678. [[CrossRef](#)]

28. Kamtchueng, B.T.; Fantong, W.Y.; Wirmvem, M.J.; Tiodjio, R.E.; Takounjou, A.F.; Ndam Ngoupayou, J.R.; Kusakabe, M.; Zhang, J.; Ohba, T.; Tanyileke, G.; et al. Hydrogeochemistry and quality of surface water and groundwater in the vicinity of Lake Monoun, West Cameroon: Approach from multivariate statistical analysis and stable isotopic characterization. *Environ. Monit. Assess.* **2016**, *524*, 1–24. [[CrossRef](#)] [[PubMed](#)]
29. Freeze, R.A.; Cherry, J.A. *Groundwater*; Prentice Hall: Englewood Cliffs, NJ, USA, 1979; p. 604.
30. Takem, G.E.; Kuitcha, D.; Ako, A.A.; Mafany, G.T.; Takounjou-Fouepe, A.; Ndjama, J.; Ntchancho, R.; Ateba, B.H.; Chandrasekharam, D.; Ayonghe, S.N. Acidification of shallow groundwater in the unconfined sandy aquifer of the city of Douala, Cameroon, Western Africa: Implications for groundwater quality and use. *Environ. Earth Sci.* **2015**, *61*, 287–298. [[CrossRef](#)]
31. Wirmvem, M.J.; Ohba, T.; Fantong, W.Y.; Ayonghe, S.N.; Suila, J.Y.; Asaah, A.N.E.; Tanyileke, G.; Hell, J.V. Hydrogeochemistry of shallow groundwater and surface water in the Ndop plain, NorthWest Cameroon. *Afr. J. Environ. Sci. Technol.* **2013**, *7*, 518–530.
32. Ako, A.A.; Shimada, J.; Hosono, T.; Ichianagi, K.; Nkeng, G.E.; Fantong, W.Y.; Takem, G.E.E.; Njila, N.R. Evaluation of groundwater quality and its suitability for drinking, domestic, and agricultural uses in the Banana Plain (Mbanga, Njombe, Penja) of the Cameroon Volcanic Line. *Environ. Geochem. Health* **2011**, *33*, 559–575. [[CrossRef](#)] [[PubMed](#)]
33. World Health Organization (WHO). *Guidelines for Drinkingwater Quality: Training Pack*; WHO: Geneva, Switzerland, 2004.
34. Piper, A.M. A graphical interpretation of water-analysis. *Trans. Am. Geophys. Union* **1944**, *25*, 914–928. [[CrossRef](#)]
35. Hem, J.D. *Study and Interpretation of the Chemical Characteristics of Natural Water*; U.S Geological Survey Water-Supply Paper; U.S Geological Survey: Reston, VA, USA, 1989; p. 272.
36. Nesbitt, H.W.; Wilson, R.E. Recent chemical weathering of basalts. *Am. J. Sci.* **1992**, *292*, 740–777. [[CrossRef](#)]
37. Herczeg, A. Can major ion chemistry be used estimated groundwater residence time in basaltic aquifer? In Proceedings of the 9th International Symposium on Water–Rock Interaction, Taupo, New Zealand, 30 March–3 April 1998; Cidu, R., Ed.; Balkema: Rotterdam, The Netherlands, 1998; pp. 529–532.
38. Subramani, T.; Rajmohan, N.; Elango, L. Groundwater geochemistry and identification of hydrogeochemical processes in hard rock region, Southern India. *Environ. Monit. Assess.* **2010**, *162*, 123–137. [[CrossRef](#)] [[PubMed](#)]
39. Tanyileke, G.; Kusakabe, M.; Evans, W.C. Chemical and isotopic characteristics of fluids along the Cameroon Volcanic Line, Cameroon. *J. Afr. Earth Sci.* **1996**, *22*, 433–441. [[CrossRef](#)]
40. Ako, A.A.; Shimada, J.; Hosono, T.; Kagabu, M.; Ayuk, A.R.; Nkeng, G.E.; Takem, G.E.E.; Takounjou, A.L.F. Spring water quality and usability in the Mount Cameroon area revealed by hydrogeochemistry. *Environ. Geochem. Health* **2012**. [[CrossRef](#)] [[PubMed](#)]
41. Appelo, C.A.J.; Postma, D. *Geochemistry, Groundwater, and Pollution*, 2nd ed.; Balkema Publishers: Rotterdam, The Netherlands, 2005; p. 649.
42. Demlie, M.; Wohnlich, S.; Wisotzky, F.; Gizaw, B. Groundwater recharge, flow and hydrogeochemical evolution in a complex volcanic aquifer system, central Ethiopia. *Hydrogeol. J.* **2007**, *15*, 1169–1181. [[CrossRef](#)]
43. Gibbs, R.J. Mechanisms controlling world water chemistry. *Science* **1970**, *17*, 1088–1090. [[CrossRef](#)] [[PubMed](#)]
44. Korjinski, D. Differential mobility of component of metasomatic zoning in metamorphism. In Proceedings of the 18th International Geology Congress, London, UK, 25 August–1 September 1948; pp. 5–7.
45. Pédro, G. Essai sur la caractérisation géochimique des différents processus zonaux résultant de l’altération des roches superficielles (cycle alumino-silicique). *C. R. Acad. Sci.* **1966**, *262*, 1828–1831.
46. Claquin, T.; Schulz, M.; Balkanski, Y. Modeling the mineralogy of atmospheric dust sources. *J. Geophys. Res.* **1999**, *104*, 22243–22256. [[CrossRef](#)]
47. Caquineau, S.; Gaudichet, A.; Gomes, L.; Legrand, M. Mineralogy of Saharan dust transported over northwestern tropical Atlantic Ocean in relation to source regions. *J. Geophys. Res.* **2002**, *107*. [[CrossRef](#)]
48. Journet, E.; Balkanski, Y.; Harrison, S.P. A new data set of soil mineralogy for dust-cycle modeling. *Atmos. Chem. Phys.* **2014**, *14*, 3801–3816. [[CrossRef](#)]
49. Stoch, L.; Sikora, W. Transformations of micas in the process of kaolinitisation of granite and gneisses. *Clay Clay Miner.* **1976**, *24*, 156–162. [[CrossRef](#)]
50. Matini, L.; Tathy, C.; Moutou, J.M. Seasonal groundwater quality variation in Brazzaville, Congo. *Res. J. Chem. Sci.* **2012**, *2*, 7–14.

51. Hounslow, A.W. *Water Quality Data: Analysis and Interpretation*; Lewis Publishers: Boca Raton, FL, USA, 1995; p. 416.
52. Srinivasamoorthy, K.; Chidambaram, S.; Prasanna, M.V.; Vasanthavihar, M.; Peter, J.; Anandhan, P. Identification of major sources controlling groundwater chemistry from a hard rock terrain—A case study from Mettur taluk, Salem district, Tamil Nadu. *J. Earth Syst. Sci.* **2008**, *117*, 49–58. [[CrossRef](#)]
53. Fisher, R.S.; Mulican, W.F., III. Hydrochemical evolution of sodium-sulfate and sodium-chloride groundwater beneath the Northern Chihuahuan Desert, Trans-Pecos, Texas, USA. *Hydrogeol. J.* **1997**, *10*, 455–474. [[CrossRef](#)]
54. Jankowski, J.; Acworth, R.I.; Shekarforoush, S. Reverse ionexchange in deeply weathered porphyritic dacite fractured aquifer system, Yass, New South Wales, Austria. In *Proceedings of the 9th International Symposium on Water–Rock Interaction, Taupo, New Zealand, 30 March–3 April 1998*; Arehart, G.B., Hulston, J.R., Eds.; Balkema: Rotterdam, The Netherlands, 1998; pp. 243–246.
55. Kumar, M.; Kumari, K.; Ramanathan, A.I.; Saxena, R. A comparative evaluation of groundwater suitability for irrigation and drinking purposes in two intensively cultivated districts of Punjab, India. *Environ. Geol.* **2007**, *53*, 553–574. [[CrossRef](#)]
56. Fantong, W.Y.; Satake, H.; Ayonghe, S.N.; Aka, F.T.; Asai, K. Hydrogeochemical controls and usability of groundwater in the semi-arid Mayo Tsanaga River Basin: Far north province, Cameroon. *Environ. Geol.* **2009**, *58*, 1281–1293. [[CrossRef](#)]
57. Hendry, M.J.; Wassenaar, L.L. Controls on the distribution of majors ions in pore waters of a thick surficial aquitard. *Water Resour. Res.* **2000**, *36*, 503–513. [[CrossRef](#)]



© 2017 by the authors. Licensee MDPI, Basel, Switzerland. This article is an open access article distributed under the terms and conditions of the Creative Commons Attribution (CC BY) license (<http://creativecommons.org/licenses/by/4.0/>).